Applied Catalysis B: Environmental 198 (2016) 303–310

Contents lists available at ScienceDirect

Applied Catalysis B: Environmental

journal homepage: www.elsevier.com/locate/apcatb

# Novel photothermocatalytic synergetic effect leads to high catalytic activity and excellent durability of anatase $TiO_2$ nanosheets with dominant {001} facets for benzene abatement

Lu Ren, Mingyang Mao, Yuanzhi Li*, Lan Lan, Zhen Zhang, Xiujian Zhao

*State Key Laboratory of Silicate Materials for Architectures, Wuhan University of Technology, 122 Luoshi Road, Wuhan 430070, PR China*

ARTICLE INFO

*Article history:*
Received 25 April 2016
Received in revised form 23 May 2016
Accepted 28 May 2016
Available online 31 May 2016

*Keywords:*
Anatase $TiO_2$ nanosheets
{001} facets
Photothermocatalytic
Benzene oxidation
Catalytic durability

ABSTRACT

We studied the effect of reaction temperature on the photocatalytic activity of anatase $TiO_2$ nanosheets with dominant {001} facets for the gas-phase photocatalytic oxidation of recalcitrant and carcinogenic benzene. It is found that the photocatalytic activity of the $TiO_2$ nanosheets significantly enhances with increasing reaction temperature from room temperature to 240, and 290 °C. Meanwhile, obvious thermocatalytic oxidation of benzene is observed on the $TiO_2$ nanosheets in the dark when the reaction temperature increases above 240 °C. The photothermocatalytic activity ($CO_2$ production rate, $r_{CO2\text{-}ptc}$) of the $TiO_2$ nanosheets at 240 or 290 °C under the irradiation of an Hg lamp is much higher than the summation of the photocatalytic activity ($r_{CO2\text{-}pc}$) with the same UV light intensity at room temperature and thermocatalytic activity ($r_{CO2\text{-}tc}$) at the same reaction temperature in the dark. This result indicates the presence of a photothermocatalytic synergetic effect between the photocatalysis and the thermocatalysis on the $TiO_2$ nanosheets, thus significantly increasing the catalytic activity. The photothermocatalytic synergetic effect is further verified by in-situ FTIR spectra with CO as probe molecule: active species produced by photogenerated electrons and holes accelerate the thermocatalytic oxidation on the $TiO_2$ nanosheets, thus significantly increasing the catalytic activity. Just by coating the sample of $TiO_2$ nanosheets on the surface of the Hg lamp, we realized highly efficient photothermocatalytic oxidation of benzene with utilizing UV light and heating effect of infrared light from the He lamp without using additional heater. Under such photothermocatalytic condition, the photothermocatalytic activity ($r_{CO2\text{-}ptc}$) of the $TiO_2$ nanosheets increased by 42.3 times as compared to the photocatalytic activity ($r_{CO2\text{-}pc}$) at room temperature with the same Hg lamp, and the $TiO_2$ nanosheets exhibit excellent durability for benzene oxidation.



## 1. Introduction

Every year millions of tons of volatile organic compounds (VOCs) are emitted from various industrial processes related to the production and utilization of paint, fine chemical, petrochemicals, etc. VOCs as major air pollutants in indoor and polluted urban atmosphere are harmful to human health as well as air environment. Efficient VOCs abatement technologies with low cost and low energy consumption are urgently needed. Photodegradation of VOCs based on various photocatalysts has been attracting intensive interests as it provides a promising low energy consumption technology for VOCs abatement [1–5]. Among various photocatalysts for VOCs abatement, nanostructured $TiO_2$ is regarded as one of the most efficient UV responsive photocatalysts [6–15]. However, two major drawbacks greatly constraint its wide application in VOCs abatement. One is its quick deactivation due to the recalcitrant carbonaceous intermediates desposited on the surface of $TiO_2$ during the photocatalytic process [16–19]. Another is its low photocatalytic efficiency due to the quick recombination of photogenerated electrons and holes [14,20]. Persistent works have been devoted to resolve the two problems. The reported strategies of improving photocatalytic durability of $TiO_2$ include: depositing noble metal nanoparticles (e.g. Pt, Rh, etc.) on $TiO_2$ [21,22], forming $TiO_2$ nanocomposites such as Ag-AgBr-$TiO_2$, preparing ordered $TiO_2$ nanotubes [23] and anatase/brookite/rutile tri-crystalline $TiO_2$ [24], so on. However, according to photocatalytic reaction pathways triggered by photogenerated electrons and holes on semiconductors, the accumulation of the recalcitrant carbonaceous intermediates on the surface of photocatalyst, resulting in gradual deactivation, is unavoidable especialy for the photodegrdation of recalcitrant aromatic VOCs such as benzene, toluene [25], etc. Thus, it is very difficult to realize a long-term durability of the photocat-

* Corresponding author.
*E-mail address:* liyuanzhi66@hotmail.com (Y. Li).

http://dx.doi.org/10.1016/j.apcatb.2016.05.073
0926-3373/

alyst for VOCs abatement. Usually, regeneration of a deactivated photocatalyst is necessary [21]. For example, although Choi et al. improved the durability for toluene photodegradation by preparing ordered $TiO_2$ nanotubes (TNT) to reduce the mass transfer limitation of $O_2$ molecules, thus hindering the accumulation of carbonaceous residues on TNT surface, TNT still experienced gradual deactivation after recycled several times [26].

The reported strategies of increasing photocatalytic efficiency of $TiO_2$ inculde: increasing the specific surface area by synthesizing mesoporous or macro-porous $TiO_2$ [27,28], increasing the separation efficiency of photogenerated electrons and holes by forming rutile/anatase junctions [29], decreasing the relative concentration ratio of bulk defects to surface defects in $TiO_2$ nanocrystals [14], and forming nanocomposites such $TiO_2$/graphene [30,31], preparing $TiO_2$ nanocrystal with high energy facets (e.g. {001}) [15,32–35], etc. Among the strategies, the photodegradation of VOCs based on anatase $TiO_2$ nanosheets with dominant {001} facets has attracted intensive interests due to their unique physicochemical properties such as active unsaturated Ti atoms, high surface energy, etc. [36–42]. It has been reported that the photocatalytic activity of $TiO_2$ with dominant {001} facets for VOCs abatement is affected by many factors such as the percentage of the exposed {001} facets [43], adsorption capacity of VOCs, amount of F existed on the {001} that affects the $O_2$ adsorption [32], and the interaction between reactant and $TiO_2$ [15] etc. Several research groups reported that $TiO_2$ with dominant {001} facets showed higher photocatalytic activity than $TiO_2$ with exposed stable{101} facets for the gas-phase photodegradation of VOCs such as toluene, acetaldehyde, acetone, etc. [43,44]. However, in order to realize the potential application of $TiO_2$ with dominant {001} facets in VOCs abatement, its photocatalytic activity needs to be considerably enhanced, and its photocatalytic deactivation for the photodegradation of VOCs especially with higher concentration needs to be resolved [35].

Therefore, it is highly desirable but great challenging to find a novel strategy of improving the photocatalytic durability as well as photocatalytic activity of $TiO_2$ with dominant {001} facets. Recently, we found that a photothermocatalytic synergetic effect between photocatalysis on $TiO_2$ and thermocatalysis on $CeO_2$ [45] or manganese oxide [13] significantly enhanced the catalytic activity and durability for VOCs abatement. It is unclear whether there is a photothermocatalytic synergetic effect on $TiO_2$ with dominant {001} facets. Herein, for the first time, we find a synergetic effect between the photocatalysis and the thermocatalysis on the $TiO_2$ nanosheets with dominant {001} facets that can significantly enhance the photocatalytic activity for the gas-phase oxidation of the recalcitrant and carcinogenic benzene. Just by coating the sample of $TiO_2$ nanosheets on the surface of a high pressure Hg lamp, we realize highly efficient photothermocatalytic oxidation of benzene with utilizing UV light and heating effect of infrared light from the Hg lamp without using additional heater. Under such photothermocatalytic condition, the photothermocatalytic activity ($r_{CO2\text{-}ptc}$) of the $TiO_2$ nanosheets increases by 42.3 times as compared to the photocatalytic activity ($r_{CO2\text{-}pc}$) at room temperature with the same Hg lamp, and the $TiO_2$ nanosheets exhibit excellent durability for benzene oxidation. We reveal the origin of the photothermocatalytic synergetic effect: active species produced by photogenerated electrons and holes accelerate the thermocatalytic oxidation on the $TiO_2$ nanosheets, thus significantly increasing the catalytic activity.

## 2. Experimental

### 2.1. Preparation

Anatase $TiO_2$ nanosheets with dominant {001} facets were prepared according to our precious work [15]. 25 mL of $Ti(OBu)_4$ and 3 mL of 40 wt.% hydrofluoric acid solution were mixed in a 100 mL Teflon bottle, and sealed tightly in a stainless-steel autoclave. The autoclave was placed in an electrical oven, heated to 180 °C, and kept at the temperature for 24 h. After the autoclave was cooled to room temperature, the resulting precipitate was washed with ethanol, then washed with 0.1 mol $L^{-1}$ NaOH aqueous solution, finally washed with distilled water to remove fluorine in the $TiO_2$ precipitate, filtered, and dried in an oven at 80 °C for 6 h.

### 2.2. Photocatalytic activity

The photocatalytic oxidation of benzene on the $TiO_2$ sample at different temperature was tested on a closed cylindrical stainless steel gas-phase reactor (5.56 L) with a quartz window (130 mm in diameter). 0.5000 g of the $TiO_2$ sample was dispersed on a 150 mm glass dish, and put on the bottom of the reactor. The reactor covered by thermal insulation slice was put on a hot plate to control the reaction temperature. A thermocouple was put on the $TiO_2$ sample to measure the temperature. An 80 W high pressure Hg lamp was fixed above the quartz window of the reactor. The intensity of UV light from the Hg lamp on the sample, measured by an UV-A radiometer, is 1.0 mW $cm^{-2}$. Under the irradiation of the Hg lamp, after the reactor was heated to a known reaction temperature (e.g. 60 °C, 240 °C, 290 °C), 5 μL of benzene was injected into the reactor. The photocatalytic activity of the $TiO_2$ sample at room temperature was measured with the same procedure besides turning off the hot plate. Reactants and products were analyzed on a GC9560 gas chromatograph. The details of GC analysis condition are described in our previous works [46,47].

The thermocatalytic activity measurements for the oxidation of benzene were carried out at the same reactor on the hot plate to control the reaction temperature in the dark without turning on the Hg lamp.

The tests of photothermocatalytic durability were taken in a closed cylindrical stainless steel gas-phase reactor with a volume of 7.2 L. The Hg lamp was set on the inner wall of the reactor. 0.5000 g of the $TiO_2$ sample dispersed in 20 mL of ethanol, was coated on the surface of Hg lamp, and dried by an infrared lamp.

### 2.3. Photocurrent

Photocurrent measurements were carried out as follows. The $TiO_2$ powder was mixed with distilled water, and ground to slurry with an agate mortar. The $TiO_2$ slurry was uniformly spread on an ITO glass substrate (1.0 cm × 2.5 cm). Another ITO glass substrate was covered on the slurry to form an ITO/$TiO_2$ film/ITO stack, and dried at 120 °C for 3 h. The stack was placed on the bottom of a hot plate to control the temperature. The transient response of photocurrent for the ITO/$TiO_2$ film/ITO stack at different temperature was recorded under an operation voltage of 0.5 V with or without the irradiation of the Hg lamp on an electrochemical analyzer (CHI750).

### 2.4. In-situ FTIR

In-situ FTIR (Fourier transform infrared spectroscopy) was tested on a Nicolet-6700 infrared spectrometer equipped with a reaction chamber (Harrick). 0.0400 g of the $TiO_2$ sample was dispersed on the sample stage incorporated in a cartridge heater with a thermocouple in the reaction chamber. Before the test, the $TiO_2$ sample was pretreated in a flow of 5 vol% $O_2$/He (20 mL $min^{-1}$)at 200 °C for 1 h. The carrier gas was changed to a flow of high pure $N_2$ (20 mL $min^{-1}$) purified by $O_2$ absorbent (Fe/$SiO_2$), kept at 200 °C for 40 min to remove the chemisorbed water on the $TiO_2$ sample and the $CO_2$ in the chamber, and then cooled to the room temperature. The carrier gas was changed to a flow of high pure CO (20 mL $min^{-1}$)

for 10 min, and then changed to a flow of high pure $N_2$ for 20 min. After that, the flow of high pure $N_2$ was shut off. The FTIR spectra of the $TiO_2$ sample were recorded at room temperature in the dark. After 2 min UV irradiation from a Xe lamp through an optical fiber, the FTIR spectra of the $TiO_2$ sample were again recorded at room temperature. Then, the $TiO_2$ sample was heated to 240 °C in 10 min, the FTIR spectra of the $TiO_2$ sample were recorded at this temperature in the dark. After the UV irradiation for 2 min, the FTIR spectra of the $TiO_2$ sample were again recorded at 240 °C. Finally, the $TiO_2$ sample was heated from 240 to 290 °C in 10min, the FTIR spectra of the $TiO_2$ sample were recorded at this temperature in the dark. After the UV irradiation for 2 min, the FTIR spectra of the $TiO_2$ sample were again recorded at 290 °C.

## 3. Resutls and discussion

### 3.1. Effect of temperature on photocatalytic activity

Anatase $TiO_2$ nanosheets with dominant {001} facets were prepared by hydrothermal reaction of $Ti(OBu)_4$ in the presence of known amount of hydrofluoric acid at 180 °C for 24 h. The residue surface F was removed by 0.1 mol $L^{-1}$ NaOH aqueous solution washing and then by distilled water washing [15]. XRD reveals that the $TiO_2$ sample has pure anatase structure [15]. The narrow {200} peak and broad {004} peak indicate that the crystal growth is limited primarily to the [001] axis, resulting in the dominant {001} facets. SEM and TEM images confirm that the $TiO_2$ sample has morphology of nanosheets with dominant {001} facets [15]. The percentage of the exposed {001} facets is estimated by the average thickness and length to be 72.3%. XPS confirms that the surface F is removed by the washing and $Na^+$ is not detected [15]. $N_2$ adsorption-desorption experiment shows that the BET surface area is 113.1 $m^2$ $g^{-1}$ [15].

Among various VOCs, recalcitrant and carcinogenic benzene has been regarded as a priority hazardous substance for which high efficient treatment technologies are needed. Therefore, we evaluated the effect of temperature on the photocatalytic activity of the $TiO_2$ nanosheets with dominant {001} facets for benzene oxidation under the irradiation of the Hg lamp with the same UV light intensity. For the $TiO_2$ nanosheets, the time course of the concentration of benzene and $CO_2$ produced from benzene oxidation with the irradiation of the Hg lamp at different temperature was shown in Fig. 1A and 1B. At room temperature (RT), the $TiO_2$ nanosheets exhibit photocatalytic activity for the photodegradation of benzene. With the elevation of the irradiation time, the concentration of benzene decreases (Fig. 1A), accompanied with the production of $CO_2$ (Fig. 1B). The concentration of $CO_2$ produced after the irradiation for 65 min is 218.6 mg $m^{-3}$. Increasing the reaction temperature from room temperature to 60 °C leads to a slight improvement in the activity. After the irradiation for 65 min, the concentration of $CO_2$ produced increases to 368.9 mg $m^{-3}$. Surprisingly, when the reaction temperature is elevated to 240 °C, the concentration of $CO_2$ produced sharply rises to 1359.5 mg $m^{-3}$. At 290 °C, the photocatalytic activity is further enhanced and the concentration of $CO_2$ produced increases to 1639.8 mg $m^{-3}$. The photocatalytic activity at different temperature is charactered by the $CO_2$ production rate ($r_{CO2}$), which is defined as the amount of the produced $CO_2$ in 30 min per unit time and unit mass of catalyst. For convenience, the $r_{CO2}$ of the $TiO_2$ nanosheets at room temperature (photocatalytic) is denoted as $r_{CO2\text{-}pc}$. The $r_{CO2}$ of the $TiO_2$ nanosheets at higher temperature (photothermocatalytic) is denoted as $r_{CO2\text{-}ptc}$. Fig. 1C shows the $r_{CO2}$ of the $TiO_2$ nanosheets for benzene oxidation at different temperature. At room temperature, the $r_{CO2}$ of the $TiO_2$ nanosheets ($r_{CO2\text{-}pc}$) is 0.77 μmol $min^{-1}$ $g^{-1}$. Increasing the reaction temperature from room temperature to

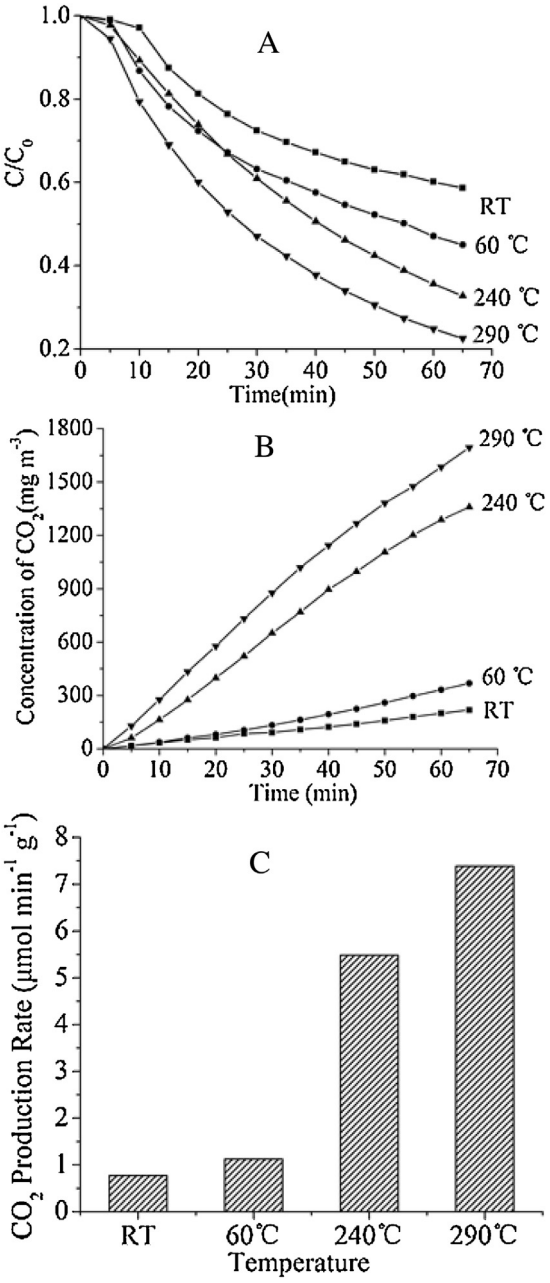


**Fig. 1.** The time course of the concentration of benzene (A), $CO_2$ produced from benzene oxidation (B), and $CO_2$ production rate ($r_{CO2}$) for benzene oxidation (C) on $TiO_2$ sample with UV irradiation at different temperature.

60 °C leads to a slight incease in $r_{CO2}$ to 1.12 μmol $min^{-1}$ $g^{-1}$. Interestingly, when the reaction temperature inceases to 240 °C, the $r_{CO2}$ greatly improves to 5.49 μmol $min^{-1}$ $g^{-1}$, which is 7.1 times higher than the $r_{CO2\text{-}pt}$ at room temperature. When the reaction temperature further increase to 290 °C, the $r_{CO2\text{-}ptc}$ increases to 7.39 μmol $min^{-1}$ $g^{-1}$. Compared to the $r_{CO2}$ at room temperature with the same light intensity, the $r_{CO2\text{-}ptc}$ at 290 °C increases by 9.6 times. The result indicates that increasing temperature can significantly improve the photocatalytic activity of the $TiO_2$ nanosheets with dominant {001} facets.

### 3.2. Photocurrent

Why does the photocatalytic activity of the $TiO_2$ nanosheets significantly improve with the elevation of the reaction temperature,

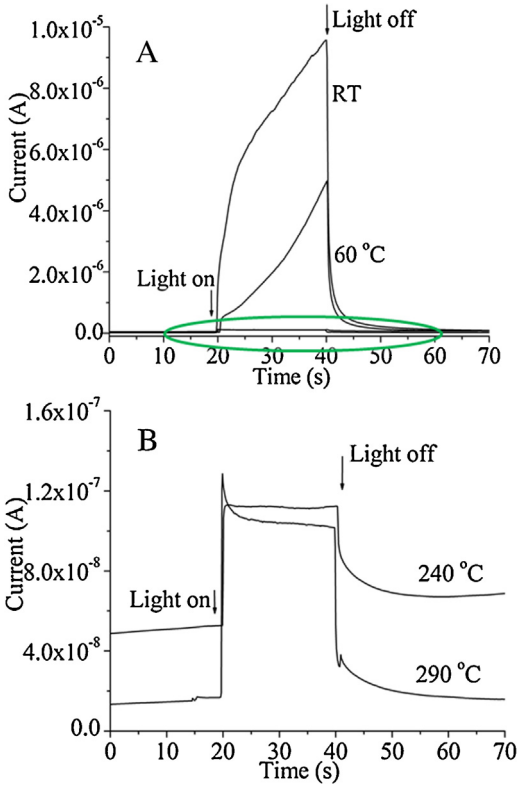


**Fig. 2.** The transient response of the photocurrent of $TiO_2$ sample under UV irradiation at different temperature (A) and the amplification of the green circle in Fig. 2A (B). (For interpretation of the references to colour in this figure legend, the reader is referred to the web version of this article.)

especially above 240 °C? It is well known that the photocatalytic activity of photocatalysts (e.g. $TiO_2$) is mainly determined by the separation efficiency of photogenerated electrons and holes, which can be characterized by the photocurrent measurement: the higher the photocurrent is, the higher the *e–h* separation efficiency is, and thus, the higher the photocatalytic activity is [14,15,48,49]. Therefore, to clarify the origin of the photocatalytic enhancement with the elevation of temperature, we investigated the effect of temperature on the photocurrent of the $TiO_2$ nanosheets. Fig. 2 shows the transient response of the photocurrent of the $TiO_2$ nanosheets under the irradiation of the Hg lamp at different temperature. As shown in Fig. 2A, at room temperature, the $TiO_2$ nanosheets exhibit considerable photocurrent response under the UV irradiation. Increasing the measurement temperature to 60 °C leads to a quick decrease in the photocurrent. When the temperature further increases to 240 °C, a dramatic decrease in the photocurrent of the $TiO_2$ nanosheets is observed (Fig. 2B). The dramatic decrease in the photocurrent is attributed to the decrease in the mobility of charge carrier due to acoustic wave scattering ($\mu_a$) with the elevation of temperature ($\mu_a$ is proportional to $T^{-3/2}$) and the enhanced recombination of photogenerated *e–h* with the elevation of temperature [3,50,51]. The dramatic decrease in the photocurrent indicates that the *e–h* separation efficiency of the $TiO_2$ nanosheets dramatically decreases with the elevation of temperature. When the temperature increases from 240 to 290 °C, the photocurrent of the $TiO_2$ nanosheets slightly increases. The slight increase in photocurrent with the elevation of temperature from 240 to 290 °C is attributed to the increase in the mobility of charge carrier due to ionized impurity scattering ($\mu_i$) with the elevation of temperature ($\mu_i$ is proportional to $T^{3/2}$) [3,51].

According to the conventional photocatalysis principle on semiconductors, the dramatic decrease in the separation efficiency of

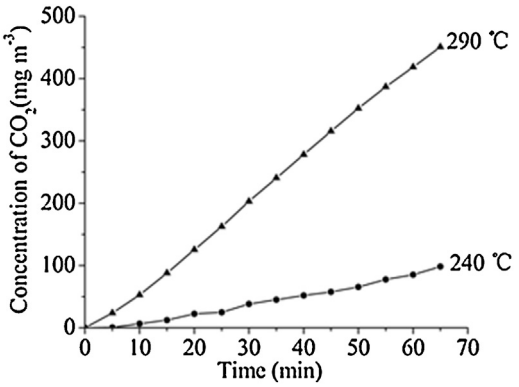


**Fig. 3.** The time course of the concentration of $CO_2$ produced from benzene oxidation without UV irradiation at different temperature.

the $TiO_2$ nanosheets with increasing temperature should result in a significant reduction in the photocatalytic activity [14,52]. Unexpectedly, as shown in Fig. 1, the photocatalytic activity of the $TiO_2$ nanosheets significantly increases with the elevation of temperature from room temperature to 290 °C. This result reveals that there probably exists a novel effect or mechanism accounting for the significant enhancement in the photocatalytic activity with the elevation of temperature

### 3.3. Thermocatalytic activity at different temperature

Usually, metal oxides such as $CeO_2$ [45,53], $MnO_2$ [47,54], $TiO_2$ [13] have thermocatalytic oxidation activity at higher temperature in the dark. Therefore, to clarify whether thermocatalytic oxidation could occur on the $TiO_2$ nanosheets and the thermocatalysis could contribute to the high catalytic activity of the $TiO_2$ nanosheets under the irradiation of the Hg lamp at higher temperature (Fig. 1), we measured thermocatalytic activity of the $TiO_2$ nanosheets for benzene oxidation in the dark at different temperature (Fig.3). At room temperature and 60 °C, no $CO_2$ is detected, indicating that benzene could not be oxidized on the $TiO_2$ nanosheets at room temperature and 60 °C in the dark. When the reaction temperature increases to 240 °C, benzene can be oxidized on the $TiO_2$ nanosheets, indicating that thermocatalytic oxidation occurs at this temperature. After reacted for 65 min, the concentration of $CO_2$ produced increases to 98.2 mg $m^{-3}$. At 240 °C, the $CO_2$ production rate for thermocatalytic oxidization (denoted as $r_{CO2\text{-}tc}$) is 0.32 μmol $min^{-1}$ $g^{-1}$. The thermocatalytic activity of the $TiO_2$ nanosheets at 240 °C can provide reasonable explanation why the catalytic activity under the irradiation of the Hg lamp sharply increases when the temperature increases to 240 °C. With increasing the temperature to 290 °C, the thermocatalytic activity considerably improves. After 65 min, the concentration of $CO_2$ produced increases to 450.7 mg $m^{-3}$. The $r_{CO2\text{-}tc}$ increases from 0.32 to 1.71 μmol $min^{-1}$ $g^{-1}$. It was reported that benzene oxidization on $TiO_2$ (P25) was negligible at the reaction temperature below 340 °C [13]. In striking contrast, the $TiO_2$ nanosheets with dominant {001} facets exhibit much higher thermocatalytic activity than $TiO_2$ (P25), evidenced by their obvious thermocatalytic activity for benzene oxidation even at 240 °C. This is attributed to the higher surface energy of the exposed {001} facets in the $TiO_2$ nanosheets as compared to that of the exposed {101} facets of anatase in $TiO_2$ (P25) [55]. The result suggests that the thermocatalysis on the $TiO_2$ nanosheets contributes to the high catalytic activity of the $TiO_2$ nanosheets under the irradiation of the lamp at higher temperature as shown in Fig. 1.

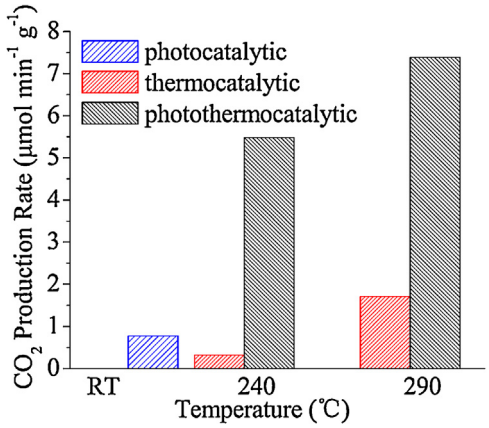


**Fig. 4.** $CO_2$ production rate ($r_{CO2}$) for benzene oxidation on $TiO_2$ sample in different reaction conditions.

### 3.4. Photothermocatalytic synergetic effect

To clarify whether the photocatalysis and thermocatalysis on the $TiO_2$ nanosheets take place independently under the irradiation of the Hg lamp at higher temperature (Fig. 1), we compare the $CO_2$ production rates for the photocatalytic ($r_{CO2\text{-}pc}$), thermocatalytic ($r_{CO2\text{-}tc}$), and photothermocatalytic ($r_{CO2\text{-}ptc}$) oxidation of benzene at different temperature (Fig. 4). If the photocatalysis and thermocatalysis on the $TiO_2$ nanosheets take place independently, at the same temperature with the same light intensity of the UV irradiation, $r_{CO2\text{-}ptc}$ of the $TiO_2$ nanosheets should be the summation of $r_{CO2\text{-}tc}$ and $r_{CO2\text{-}pc}$. As shown in Fig. 4, interestingly, the $r_{CO2\text{-}ptc}$ at 240 °C (5.49 μmol $min^{-1}$ $g^{-1}$) is 5.0 times higher than the summation of $r_{CO2\text{-}tc}$ at 240 °C (0.32 μmol $min^{-1}$ $g^{-1}$) and $r_{CO2\text{-}pc}$ at room temperature with the same light intensity of the UV irradiation (0.77 μmol $min^{-1}$ $g^{-1}$) (Fig. 4). Similar phenomena is observed at 290 °C. The $r_{CO2\text{-}ptc}$ at 290 °C (7.39 μmol $min^{-1}$ $g^{-1}$) is 3.0 times higher than the summation of $r_{CO2\text{-}tc}$ at 290 °C (1.71 μmol $min^{-1}$ $g^{-1}$) and $r_{CO2\text{-}pc}$ at room temperature with the same light intensity of the UV irradiation (0.77 μmol $min^{-1}$ $g^{-1}$) (Fig. 4). This result clearly indicates that there is a synergetic effect between the photocatalytic and thermocatalytic oxidation on the $TiO_2$ nanosheets under the irradiation of the Hg lamp at the temperature above 240 °C as illustrated in Scheme 1:

With the UV irradiation form the Hg lamp, electrons ($e$) in the valence band of the $TiO_2$ nanosheets is excited to the conduction band, leaving holes ($h$) at the valence band edge [14,15,56]. The photogenerated charge carriers migrate to the surface of $TiO_2$ to initiate various redox reactions. Because the redox potential of $e$ (−0.18 V vs NHE at pH = 1) is lower than that of $O_2$ (e.g. $O_2/O_2^-$ −0.16 V vs NHE), the photogenerated electrons reduce $O_2$ to produce $O_2^-$ active oxygen [52,57,58]. The photogenerated holes oxidize the surface $H_2O$ or hydroxyl group to form hydroxyl radical (•OH) due to the higher redox potential of $h$ (3.02 V vs NHE) than that of hydroxyl groups (e.g. OH•/$OH^-$, 1.89 V vs NHE) [52,57–59]. The photogenerated holes can also oxidize adsorbed organic molecules (e.g. benzene in the present case) to form active organic molecules (e.g. $C_6H_6^+$) due to their higher redox potential than that of organic molecules (e.g. benzene, 2.995 V vs NHE) [60]. Thus, the photodegradation of benzene facilitates. The produced $O_2^-$ and •OH can oxidize benzene and benzene$^+$ to $CO_2$ and $H_2O$.

Meanwhile, the $TiO_2$ nanosheets also demonstrate thermocatalytic activity at higher temperature as discussed above. It has been widely accepted that the thermocatalytic oxidation of organic or reducible molecule on metal oxides (e.g. $CeO_2$, $MnO_2$, $TiO_2$, etc.) follows the Mars-van Krevelen mechanism [47,53,54,61]: Organic or reducible molecule adsorbed on metal oxide (e.g. $TiO_2$) is oxidized by the surface oxygen in $TiO_2$, and then the reduced metal oxide (e.g. $TiO_{2-x}$) is subsequently re-oxidized by gaseous oxygen [17].

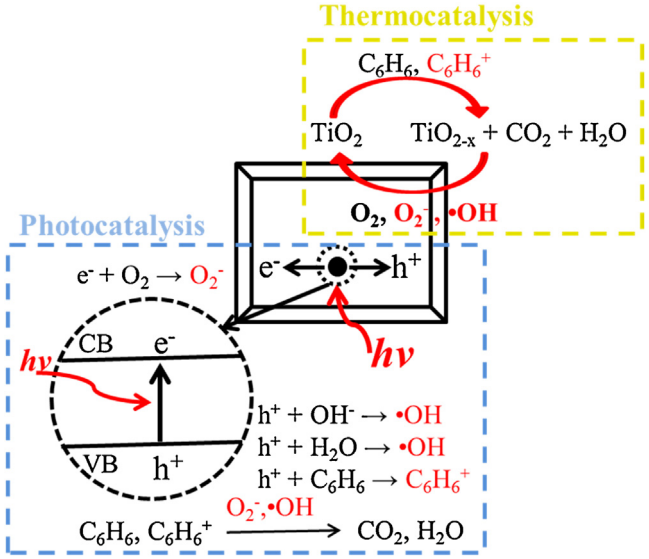


**Scheme 1.** Schematic illustration of the photothermocatalytic synergetic effect between the photocatalysis and thermocatalysis on the $TiO_2$ sample.

The active benzene (e.g. $C_6H_6^+$) formed by photocatalysis on $TiO_2$ is more active than benzene according to molecular orbital theory because the electron number in the bonding molecular orbital of $C_6H_6^+$ is less than that of benzene [62]. Thus, compared to the reduction of $TiO_2$ by benzene in the thermocatalysis in the dark, under the UV irradiation from the Hg lamp, the photogenerated active benzene (e.g. $C_6H_6^+$) can accelerate the reduction of $TiO_2$ (Scheme 1). The active oxygen (e.g. $O_2^-$) and hydroxyl radical (•OH) formed by the photocatalysis on $TiO_2$ are more active than gas-phase oxygen ($O_2$) in the thermocatalysis on $TiO_2$. Thus, compared to the re-oxidation of the reduced titania ($TiO_{2-x}$) by $O_2$ in the thermocatalysis in the dark, under the UV irradiation from the Hg lamp, the photogenerated active oxygen (e.g. $O_2^-$) and hydroxyl radical (•OH) can accelerate the oxidation of $TiO_{2-x}$ (Scheme 1). Under the UV irradiation from the Hg lamp at higher temperature (e.g. 240, 290 °C), the photothermocatalytic synergetic effect between the photocatalysis and thermocatalysis on $TiO_2$ accelerates the Mars-van Krevelen redox cycle between $TiO_2$ and $TiO_{2-x}$, thus significantly enhancing the catalytic activity of the $TiO_2$ nanosheets.

### 3.5. Origin of the photothermocatalytic syenergtic effect: in-situ FTIR

It is widely accepted that the reducibility of metal oxides (e.g. $MnO_2$, $CeO_2$, $TiO_2$) plays a crucial role in its thermocatalytic activity according to the Mars-van Krevelen mechanism as the reduction of metal oxides is much slower than the re-oxidation of reduced metal oxides [17,47,53,54]. In order to put insight in the origin of the photothermocatalytic synergetic effect, we investigated the effect of UV irradiation on the reduction of the $TiO_2$ nanosheets by in-situ FTIR spectra using CO as probe molecule in the absence of $O_2$ at different temperature in the dark or with the UV irradiation (*Experimental*). As shown in Fig. 5, there are two strong IR peaks and one weak IR peak around 2174, 2120, and 2062 $cm^{-1}$, which are assigned to CO linearly adsorbed on the different sites of the $TiO_2$ nanosheets [63]. The board peak around 2361 $cm^{-1}$ is attributed to the asymmetric stretch of $CO_2$. At room temperature, compared to the FTIR spectra of the $TiO_2$ nanosheets in the dark, the weak $CO_2$ IR peak due to

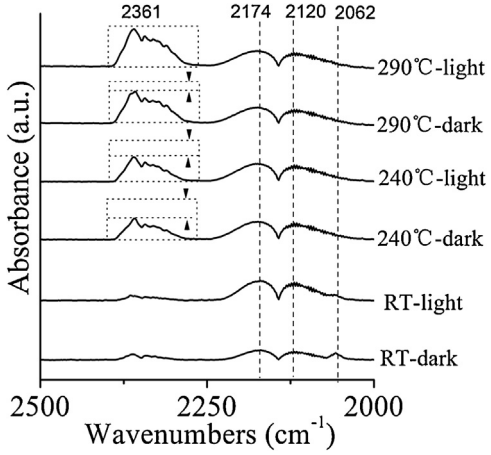


**Fig. 5.** The evolution of the in-situ FTIR spectra CO adsorbed on the pretreated $TiO_2$ nanosheets at different temperature in the dark and with the UV irradiation for 2 min: dotted box represents scale bar, RT represents room temperature.

the residue $CO_2$ in the in-situ FTIR chamber has no obvious change after irradiation for 2 min. This result suggests that CO could not be oxidized by the surface lattice oxygen in the $TiO_2$ nanosheets in the dark as well as with the UV irradiation at room temperature. When the temperature is elevated to 240 °C in the dark, a strong broad $CO_2$ peak is observed, indicating the oxidation of CO by the surface lattice oxygen in the $TiO_2$ nanosheets:

$$TiO_2 + xCO \rightarrow TiO_{2-x} + xCO_2$$

Interestingly, at 240 °C, the UV irradiationonly for 2 min gives rise to an apparent enhancement in the $CO_2$ peak intensity as compared to that in the dark. This result indicates that the UV irradiation can accelerate the oxidation of CO by the surface lattice oxygen in the $TiO_2$ nanosheets. The reason is as follows: under the UV irradiation, the photogenerated hole ($h$) on the $TiO_2$ nanosheets reacts with CO to form active CO (e.g. $CO^+$) due to the higher redox potential of $h$ than that of CO (0.64 V vs RHE on Pt electrode) [64]. The active CO (e.g. $CO^+$) is more active than CO according to molecular orbital theory as the electron number in the bonding molecular orbital of $CO^+$ is less than that of CO [64]. Thus, compared to the reduction of $TiO_2$ by CO, the active CO (e.g. $CO^+$) accelerates the reduction of the $TiO_2$ nanosheets:

$$h^+ + CO \rightarrow CO^+$$

$$TiO_2 + xCO \rightarrow TiO_{2-x} + xCO_2$$

$$TiO_2 + xCO^+ \rightarrow TiO_{2-x} + xCO_2$$

when the temperature is elevated from 240 to 290 °C in the dark, the $CO_2$ peak intensity is further enhanced, which is attributed to the promotion of the oxidation of CO by the surface lattice oxygen in the $TiO_2$ nanosheets with the elevation of temperature. Similarly, at 290 °C, the UV irradiation only for 2 min leads to an apparent enhancement in the $CO_2$ peak intensity as compared to that in the dark. This result further confirms that the photogenerated active species (e.g. $CO^+$, $C_6H_6^+$) by the photocatalysis on $TiO_2$ upon the UV irradiation can accelerate the oxidation of CO or benzene by the surface lattice oxygen in $TiO_2$ at higher temperature, thus significantly promoting the catalytic activity as illustrated in Scheme 1.

### 3.6. Photothermocatalytic activity

As discussed above, in order to realize the photothermocatalytic synergetic effect for efficient VOCs abatement on the $TiO_2$ nanosheets, the $TiO_2$ nanosheets must be heated to a certain temperature (e.g. 240 °C) at which the thermocatalytic oxidation can take place. If an additional heater is used, it will lead to high energy consumption, which hinders the potential application for VOCs abatement. Is it possible to realize the photothermocatalytic synergetic effect for efficient VOCs abatement without using additional heater? Actually, the Hg lamp as a typical light source in various photocatalytic tests not only emits UV light, but also emits visible and infrared light. The heating effect of the emitted infrared light leads to a quick increase in the surface temperature of the Hg lamp. Therefore, we coated the sample of the $TiO_2$ nanosheets on the surfaces of the Hg lamp. Thus, the sample of the $TiO_2$ nanosheets is excited by the UV light from the Hg lamp, and its surface temperature quickly increases to an equilibrium temperature about 290 °C (Fig. S1) due to the heating effect of the infrared light from the Hg lamp. Under such photothermocatalytic condition, benzene was rapidly oxidized with the evolution of the irradiation time, accompanied with a quick increase in the concentration of $CO_2$ produced (Fig. 6A and B). Only after the irradiation for 20 min, benzene is completely degraded and the concentration of $CO_2$ produced increases to 2103.7 mg $m^{-3}$. In this case, the $r_{CO2\text{-}ptc}$ of the $TiO_2$ nanosheets is as high as 32.59 μmol $min^{-1}$ $g^{-1}$, which is 42.3 times higher than the $r_{CO2\text{-}pc}$ at room temperature using the same Hg lamp (0.77 μmol $min^{-1}$ $g^{-1}$), and 4.4 times higher than the $r_{CO2\text{-}ptc}$ at 290 °C using the same Hg lamp and additional heater (7.39 μmol $min^{-1}$ $g^{-1}$) as shown in Fig. 1. By this facile strategy of coating the $TiO_2$ nanosheets on the surface of the Hg lamp, we realize highly efficient synergetic photothermocatalytic oxidation of benzene without using additional heater.

We evaluated the durability of the $TiO_2$ nanosheets coated on the surface of the Hg lamp for benzene oxidation. After the sample of the $TiO_2$ nanosheets was recycled for 30 times, its photothermocatalytic activity remained unchanged (Fig. 6B). This result indicates that under such photothermocatalytic condition, the $TiO_2$ nanosheets exhibit excellent durability. After the durability test, the used sample of the $TiO_2$ nanosheets was scratched from the surface of the Hg lamp, and characterized by FTIR. As shown in Fig. 7, the used sample of the $TiO_2$ nanosheets has the almost same FTIR spectra as the fresh sample of the $TiO_2$ nanosheets and no carbonaceous byproducts are detected by FTIR, which account for the excellent durability of the $TiO_2$ nanosheets under such photothermocatalytic condition. Compared to the fresh $TiO_2$ sample, there is a slight decrease in the broad peak intensity in 3000–3600 $cm^{-1}$ for the used $TiO_2$ sample, which is attributed to the desorption of hydroxyl group on the $TiO_2$ sample during the photothermocatalytic process at higher temperature (~290 °C, Fig. S1).

## 4. Conclusion

In summary, the photocatalytic activity of $TiO_2$ nanosheets with dominant {001} facets for the gas-phase photocatalytic oxidation of benzene significantly enhances with increasing reaction temperature. Meanwhile, obvious thermocatalytic oxidation of benzene is observed on the $TiO_2$ nanosheets in the dark when the reaction temperature increased above 240 °C. The significant enhancement in the catalytic activity is attributed to a synergetic effect between the photocatalysis and the thermocatalysis on the $TiO_2$ nanosheets: active species produced by photogenerated electrons and holes accelerate the thermocatalytic oxidation on the $TiO_2$ nanosheets, thus significantly increasing the catalytic activity. Just by coating the sample of $TiO_2$ nanosheets on the surface of the Hg lamp, we realize highly efficient photothermocatalytic oxidation of benzene with utilizing UV light and heating effect of infrared light from the Hg lamp without using additional heater. Under such photothermocatalytic condition, the $TiO_2$ nanosheets exhibit very high catalytic

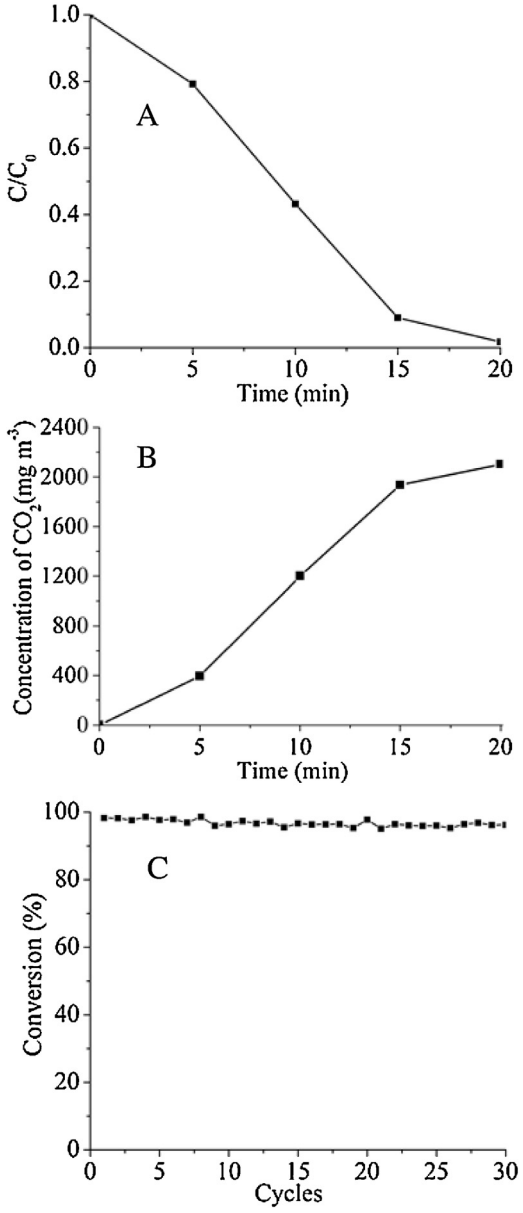


**Fig. 6.** The time course of the concentration of benzene (A) and the produced $CO_2$ (B) by the benzene oxidation on the $TiO_2$ nanosheets coated on an 80 W Hg lamp, and the durability of $TiO_2$ nanosheets for the photothermocatalytic oxidation of benzene (the initial concentration of benzene is 562 mg $m^{-3}$; reaction time of every cycle is 20 min) (C).

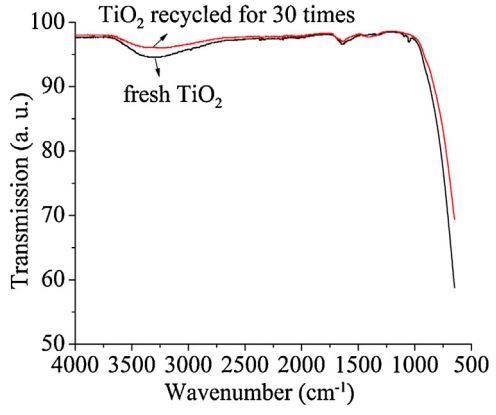


**Fig. 7.** FTIR spectra of fresh $TiO_2$ and $TiO_2$ recycled for 30 times.

activity as well as excellent durability for catalytic abatement of benzene. By this novel synergetic photothermocatalytic strategy, we succeed in resolving the major drawbacks of low photocatalytic efficiency and quick deactivation of $TiO_2$ unsolved by the conventional photocatalysis. The strategy and finding are easily applicable to other nanostructure photocatalysts, which will promote the promising application of nanostructured photocatalysts in VOCs abatement.

## Acknowledgement

This work was supported by National Natural Science Foundation of China (21273169, 21473127).

## Appendix A. Supplementary data

Supplementary data associated with this article can be found, in the online version, at http://dx.doi.org/10.1016/j.apcatb.2016.05.073.

## References

[1] H.L. Huang, H.B. Huang, Y.J. Zhan, G.Y. Liu, X.M. Wang, H.X. Lu, L. Xiao, Q.Y. Feng, D.Y.C. Leung, Appl. Catal. B: Environ. 186 (2016) 62–68.
[2] Y.C. Chen, K. Katsumata, Y.H. Chiu, K. Okada, N. Matsushita, Y.J. Hsu, Appl. Catal. A: Gen. 490 (2015) 1–9.
[3] W. Xie, Y.Z. Li, W.Q. Shi, L. Zhao, X.J. Zhao, P.F. Fang, F. Zheng, S.J. Wang, Chem. Eng. J. 213 (2012) 218–224.
[4] Y.L. Zheng, W.Z. Wang, D. Jiang, L. Zhang, X.M. Li, Z. Wang, J. Mater. Chem. A 4 (2016) 105–112.
[5] B.J. Liu, X.Y. Li, Q.D. Zhao, J. Liu, S.M. Liu, S.B. Wang, M. Tade, J. Mater. Chem. A 3 (2015) 15163–15170.
[6] C.L. Bianchia, S. Gattoa, C. Pirola, A. Naldoni, A. Di Michele, G. Cerrato, V. Crocella, V. Capucci, Appl. Catal. B: Environ. 146 (2014) 123–130.
[7] L. Zeng, Z. Lu, M.H. Li, J. Yang, W.L. Song, D.W. Zeng, C.S. Xie, Appl. Catal. B: Environ. 183 (2016) 308–316.
[8] C.H. Wang, X. T.g Zhang, Y.C. Liu, Nanoscale 6 (2014) 5329–5337.
[9] J.Y. Chen, G.Y. Li, Y. Huang, H.M. Zhang, H.J. Zhao, T.C. An, Appl. Catal. B: Environ. 123–124 (2012) 69–77.
[10] I. Jansson, S. Suárez, F. Javier Garcia-Garcia, B. Sánchez, Appl. Catal. B: Environ. 178 (2015) 100–107.
[11] R. Fiorenzaa, M. Bellarditab, L. Palmisanob, S. Scirèa, J. Mol. Catal. A 415 (2016) 56–64.
[12] A. Šuligoja, U.L. Štangara, A. Ristićb, M. Mazajb, D. Verhovšekc, N.N. Tušara, Appl. Catal. B: Environ. 184 (2016) 119–131.
[13] Y. Ma, Y.Z. Li, M.Y. Mao, J.J. Hou, M. Zeng, X.J. Zhao, J. Mater. Chem. A 3 (2015) 5509–5516.
[14] M. Kong, Y.Z. Li, X. Chen, T.T. Tian, P.F. Fang, F. Zheng, X.J. Zhao, J. Am. Chem. Soc. 133 (2011) 16414–16417.
[15] L. Ren, Y.Z. Li, J.T. Hou, J.L. Bai, M.Y. Mao, M. Zeng, X.J. Zhao, Appl. Catal. B: Environ. 181 (2016) 625–634.
[16] N. Abbas, M. Hussain, N. Russo, G. Saracco, Chem. Eng. J. 175 (2011) 330–340.
[17] Y.Z. Li, J.C. Huang, T. Peng, J. Xu, X.J. Zhao, ChemCatChem 2 (2010) 1082–1087.
[18] M.R. Rafael, C.M. Nelsonz, Catal. Today 40 (1998) 353–365.
[19] W.C. Wu, L.F. Liao, C.F. Lien, J.L. Lin, Phys. Chem. Chem. Phys. 3 (2001) 4456–4461.
[20] J.W. Tang, J.R. Durrant, D.R. Klug, J. Am. Chem. Soc. 130 (2008) 13885–13891.
[21] H. Einaga, S. Futamura, T. Ibusuki, Environ. Sci. Technol. 38 (2004) 285–289.
[22] Y.L. Chen, D.Z. Li, X.C. Wang, X.X. Wang, X.Z. Fu, Chem. Commun. (2004) 2304–2305.
[23] Y.H. Zhang, Z.R.R. Tang, X.Z. Fu, Y.J. Xu, Appl. Catal. B: Environ. 106 (2011) 445–452.
[24] K.Y. Chen, L.Z. Zhu, K. Yang, J. Environ. Sci. 32 (2015) 189–195.
[25] O. d'Hennezel, P. Pichat, D.F. Ollis, J. Photochem. Photobiol. A 118 (1998) 197–204.
[26] S.Y. Weon, W.Y. Choi, Environ. Sci. Technol. 50 (2016) 2556–2563.
[27] J.C. Yu, L.Z. Zhang, J.G. Yu, Chem. Mater. 14 (2002) 4647–4653.
[28] Y. Liu, Y. Li, Y.T. Wang, L. Xie, J. Zheng, X.G. Li, J. Hazard. Mater. 150 (2008) 153–157.
[29] T. Kawahara, Y. Konishi, H. Tada, N. Tohge, J. Nishii, S. Ito, Angew. Chem. Int. Ed. 41 (2002) 2811–2813.
[30] Y.H. Zhang, Z.R. Tang, X.Z. Fu, Y.J. Xu, ACS Nano 4 (2010) 7303–7314.
[31] Q.W. Huang, S.Q. Tian, D.W. Zeng, X.X. Wang, W.L. Song, Y.Y. Li, W. Xiao, C.S. Xie, ACS Catal. 3 (2013) 1477–1485.
[32] Y.B. Luan, L.Q. Jing, Y. Xie, X.J. Sun, Y.J. Feng, H.G. Fu, ACS Catal. 3 (2013) 1378–1385.
[33] Q.J. Xiang, K.L. Lv, J.G. Yu, Appl. Catal. B: Environ. 96 (2010) 557–564.
[34] K.L. Lv, Q.J. Xiang, J.G. Yu, Appl. Catal. B: Environ. 104 (2011) 275–281.

[35] Q.Q. Shang, X. Tan, T. Yu, Z.Y. Zhang, Y.L. Zou, S.Y. Wang, J. Colloid Interface Sci. 455 (2015) 134–144.
[36] M. Lazzeri, A. Vittadini, A. Selloni, Phys. Rev. B 63 (2001) 155409.
[37] U. Diebold, Surf. Sci. Rep. 48 (2003) 53–229.
[38] Y.Q. Dai, C.M. Cobley, J. Zeng, Y.M. Sun, Y.N. Xia, Nano Lett. 9 (2009) 2455–2459.
[39] X.G. Han, Q. Kuang, M.S. Jin, Z.X. Xie, L. Zheng, J. Am. Chem. Soc. 131 (2009) 3152–3153.
[40] C.Z. Wen, J.Z. Zhou, H.B. Jiang, Q.H. Hu, S.Z. Qiao, H.G. Yang, Chem. Commun. 47 (2011) 4400–4402.
[41] J.G. Yu, J.X. Low, W. Xiao, P. Zhou, M. Jaroniec, J. Am. Chem. Soc. 136 (2014) 8839–8842.
[42] J. Pan, G. Liu, G.Q. Lu, H.M. Cheng, Angew. Chem. Int. Ed. 50 (2011) 2133–2137.
[43] B.I. Stefanov, G.A. Niklasson, C.G. Granqvist, L. Österlund, J. Catal. 335 (2016) 187–196.
[44] M.J. Wang, F. Zhang, X.D. Zhu, Z.M. Qi, B. Hong, J.J. Ding, J. Bao, S. Sun, C. Gao, Langmuir 31 (2015) 1730–1736.
[45] M. Zeng, Y.Z. Li, M.Y. Mao, J.L. Bai, L. Ren, X.J. Zhao, ACS Catal. 5 (2015) 3278–3286.
[46] J.T. Hou, Y.Z. Li, M.Y. Mao, X.J. Zhao, Y.Z. Yue, Nanoscale 6 (2014) 15048–15058.
[47] J.T. Hou, L.L. Liu, Y.Z. Li, M.Y. Mao, H.Q. Lv, X.J. Zhao, Sci. Technol. 47 (2013) 13730–13736.
[48] L. Ren, Y.Z. Li, J.T. Hou, X.J. Zhao, C.X. Pan, ACS Appl. Mater. Interfaces 6 (2014) 1608–1615.
[49] L. Thompson, J.T. Yates Jr., Chem. Rev. 106 (2006) 4428–4453.
[50] T. Bak, J. Nowotny, M. Rekas, C.C. Sorrell, J. Phys. Chem. Solids 64 (2003) 1069–1087.
[51] E.K. Liu, B.S. Zhu, J.S. Luo, Semiconductor Physics, Publishing House of Electronics Industry, Beijing, 2008, pp. 106–126.
[52] A.L. Linsebigler, G.Q. Lu, J.T. Yates Jr., Chem. Rev. 95 (1995) 735–758.
[53] Y.Z. Li, Q. Sun, M. Kong, W.Q. Shi, J.C. Huang, J.W. Tang, X.J. Zhao, J. Phys. Chem. C 115 (2011) 14050–14057.
[54] J.T. Hou, Y.Z. Li, L.L. Liu, L. Ren, X.J. Zhao, J. Mater. Chem. A 1 (2013) 6736–6741.
[55] H.G. Yang, C.H. Sun, S.Z. Qiao, J. Zou, G. Liu, S.C. Smith, H.M. Cheng, G.Q. Lu, Nature 453 (2008) 638–642.
[56] M.A. Fox, M.T. Dulay, Chem. Rev. 93 (1993) 341–357.
[57] D.T. Sawyer, J.S. Valentine, Chem. Res. 14 (1981) 393–400.
[58] T. Tachikawa, M. Fujitsuka, T. Majima, J. Phys. Chem. C 111 (2007) 5259–5275.
[59] X.B. Chen, S.S. Mao, Chem. Rev. 107 (2007) 2891–2959.
[60] L. Luo, Y.Z. Li, J.T. Hou, Y. Yang, Appl. Surf. Sci. 319 (2014) 332–338.
[61] J.L. Yu, P.E. Savage, Environ. Sci. Technol. 34 (2000) 3191–3198.
[62] G.D. Zhou, Y.L. Duan, Structural Chemistry, Peking University Press, Peking, China, 2008, 1-363.
[63] Y.Z. Li, B.L. Xu, Y.N. Fan, N.Y. Feng, A.D. Qiu, J.W. Miao, J. He, H.P. Yang, Y. Chen, J. Mol. Catal. A 216 (2004) 107–114.
[64] R. Ianniello, V.M. Schmidt, U. Stimming, J. Super, A. Wallau, Electrochim. Acta 39 (1994) 1863–1869.